

The Electron Spectrum in 3C 279 and the Observed Emission Spectrum

Masaaki Kusunose^{1,2}, Fumio Takahara³, and Tomohiro Kato^{1,4}

ABSTRACT

The emission mechanisms of the blazar 3C 279 are studied by solving the kinetic equations of electrons and photons in a relativistically moving blob. The γ -ray spectral energy distribution (SED) is fitted by inverse Compton scattering of external photons. The bulk Lorentz factor of the emitting blob is found to be ~ 25 , and the magnetic field is found to be ~ 0.3 G. GeV γ -rays are well explained by inefficiently cooled electrons because of the Klein-Nishina effects. The electron spectrum is not a broken power law with a steeper spectrum above a break energy, which is often used to fit the observed SED. The kinetic energy density of the nonthermal electrons dominates the magnetic energy density; this result is qualitatively the same as that for TeV blazars such as Mrk 421 and Mrk 501. The γ -ray luminosity of 3C 279 is often observed to increase rapidly. We show that one of the better sampled γ -ray flares can be explained by the internal shock model.

Subject headings: quasars: general — quasars: individual (3C 279) — gamma rays: theory – radiation mechanisms: nonthermal

1. Introduction

Blazars are active galactic nuclei characterized by high energy emission and short time variability (e.g., Krolik 1999). Recent observations of blazars show that they are powerful sources of high energy emission (Ulrich, Maraschi, & Urry 1997, for review), which is

¹Department of Physics, School of Science and Technology, Kwansei Gakuin University, Sanda 669-1337, Japan

²kusunose@kwansei.ac.jp

³Department of Earth and Space Science, Graduate School of Science, Osaka University, Toyonaka 560-0043, Japan; takahara@vega.ess.esi.osaka-u.ac.jp

⁴scms1009@ksc.kwansei.ac.jp

explained by nonthermal emission by particles in relativistic jets. The emission of blazars in the GeV energy range was observed by EGRET onboard the *Compton Gamma Ray Observatory* (Thompson et al. 1995; Mukherjee et al. 1997; Hartman et al. 2001). These observations show that a large fraction of emission power from blazars is in γ -ray band (see Ghisellini et al. 1998 and Collmar 2001 for reviews).

Multiwavelength observations of 3C 279 (redshift $z = 0.538$) were performed several times (Maraschi et al. 1994; Wehrle et al. 1998; Hartman et al. 2001). Based on these results, γ -rays from 3C 279 are found to be explained by inverse Compton scattering of external UV radiation (e.g., Inoue & Takahara 1996). The sources of seed soft photons (e.g., accretion disks (Dermer & Schlickeiser 1993), broad-line regions (Sikora, Begelman, & Rees 1994), and beamed radiation reflected by broad-line region clouds (Ghisellini & Madau 1996)) have been proposed by many authors. Recently, Hartman et al. (2001) assumed soft photons from both the accretion disk and the broad-line region in order to model the emission spectra from 3C 279. Ballo et al. (2002), on the other hand, applied a broad-line region model to 3C 279.

Most emission models have assumed that electrons obey a power law (e.g., Hartman et al. 2001) or a broken power law (e.g., Inoue & Takahara 1996; Ballo et al. 2002). However, an alternative electron spectrum is possible as a result of the Klein-Nishina (K-N) effects; the smaller cooling rate due to the K-N effects makes the electron spectrum harder (Dermer & Atoyan 2002), and the emissivity of scattered photons is smaller (Georganopoulos, Kirk, & Mastichiadis 2001). Thus, the electron spectrum must be solved self-consistently, including the cooling rate in the K-N regime.

In previous work, we solved the kinetic equations of electrons and photons simultaneously in a relativistically moving blob (Li & Kusunose 2000; Kino, Takahara, & Kusunose 2002, hereafter KTK). Here we include the inverse Compton scattering of external soft photons (external Compton scattering, hereafter EC) and obtain the physical quantities for 3C 279 such as the bulk Lorentz factor, the energy densities of electrons and magnetic fields, etc.

The variability of blazars on small timescales is often observed (e.g., Wehrle et al. 1998). The time variation of fluxes is not only useful for obtaining constraints on the size of the emission region but is also important for studying the emission and particle acceleration mechanisms (Mastichiadis & Kirk 1997; Kusunose, Takahara, & Li 2000; Li & Kusunose 2000; Böttcher and Chiang 2002). Flares observed in X-ray and γ -ray regimes might be explained by the internal collisions of plasma blobs in a jet and the subsequent cooling. Without considering the details of particle acceleration after the collision, it is possible to obtain the emission spectrum by assuming that the time evolution occurs quasi-steadily. In

this Letter we present a model to explain the flare of 3C 279 observed in 1996 February.

In §2, kinetic equations for electrons and photons are described. Numerical results are given in §3 for a steady state. Results for time variability are shown in §4. Finally, §5 is devoted to the summary of our results and discussion.

2. Model

The formulation used in this Letter is the same as in Li & Kusunose (2000) and KTK. We assume that a spherical blob with radius R moves with a relativistic speed with Lorentz factor Γ . Accelerated electrons obeying a power law are injected into the blob uniformly, and they are cooled by synchrotron emission and inverse Compton scattering.

2.1. Kinetic Equations

The equation describing the time evolution of the electron number spectrum in the blob is given by

$$\frac{\partial n_e(\gamma)}{\partial t} = -\frac{\partial}{\partial \gamma} \left[\left(\frac{d\gamma}{dt} \right)_{\text{loss}} n_e(\gamma) \right] - \frac{n_e(\gamma)}{t_{e,\text{esc}}} + q(\gamma), \quad (1)$$

where γ is the Lorentz factor of electrons and $n_e(\gamma)$ is the number density of electrons per unit γ . We assume that nonthermal electrons with a power law are injected at a rate:

$$q(\gamma) = q_0 \gamma^{-p} \exp(-\gamma/\gamma_{\text{max}}) \quad \text{for } \gamma \geq \gamma_{\text{min}}, \quad (2)$$

where q_0 is the normalization. The injection is assumed to continue during a simulation with the rate given above. The energy-loss rate of electrons is denoted by $(d\gamma/dt)_{\text{loss}}$, which is due to synchrotron radiation and inverse Compton scattering. The synchrotron-loss rate is calculated by the formulation given by Robinson & Melrose (1984) for mildly relativistic electrons and by Crusius & Schlickeiser (1986) for relativistic electrons. The cooling rate of inverse Compton scattering is calculated by Coppi & Blandford (1990); although the EC process is anisotropic, we use the formulation for isotropic scattering. The value of the electron-escape timescale, $t_{e,\text{esc}}$, is set to be $3R/c$, assuming that the escape of electrons from the jet is likely due to advection. We use a method developed by Xiao, Yabe, & Ito (1996) for numerical calculations.

To obtain the isotropic photon field in the blob frame, i.e., except the EC component, we solve the following equation:

$$\frac{\partial n_{\text{ph}}(\varepsilon)}{\partial t} = \dot{n}_{\text{C}}(\varepsilon) + \dot{n}_{\text{em}}(\varepsilon) - \dot{n}_{\text{abs}}(\varepsilon) - \frac{n_{\text{ph}}(\varepsilon)}{t_{\gamma,\text{esc}}}, \quad (3)$$

where $n_{\text{ph}}(\varepsilon)$ is the photon number density per unit energy ε ; Compton scattering and synchrotron emission are denoted by $\dot{n}_{\text{C}}(\varepsilon)$ and $\dot{n}_{\text{em}}(\varepsilon)$, respectively; $\dot{n}_{\text{abs}}(\varepsilon)$ is absorption due to the self-absorption of synchrotron process and pair production; and $n_{\text{ph}}(\varepsilon)/t_{\gamma,\text{esc}}$ denotes the escape of photons (we set $t_{\gamma,\text{esc}} = R/c$). The EC component is separately calculated following Georganopoulos et al. (2001; see also Dermer & Schlickeiser 2002) because the external photons are highly anisotropic in the blob frame. We assume that in the rest frame of the central black hole, the external radiation is isotropic with energy density u_{ext} and monochromatic with energy ε_{ext} . In the blob frame, the comoving energy density of the soft photons is $u'_{\text{ext}} = u_{\text{ext}}\Gamma^2(1 + \beta_{\Gamma}^2/3)$, where $\beta_{\Gamma} = (1 - \Gamma^{-2})^{1/2}$ (Dermer & Schlickeiser 2002). On the other hand, the energy of the external photons is $\varepsilon'_{\text{ext}} \approx \Gamma\varepsilon_{\text{ext}}$.

The observed radiation is boosted by the Doppler effect characterized by the beaming factor $\mathcal{D} = [\Gamma(1 - \beta_{\Gamma} \cos \theta_{\text{obs}})]^{-1}$, where θ_{obs} is the angle between the jet propagation and the line of sight (Blandford & Königl 1979). In this Letter, we assume $\mathcal{D} = \Gamma$. The parameters to be determined are Γ , γ_{min} , γ_{max} , p , q_0 , B , R , ε_{ext} , and u_{ext} .

The comoving quantities are transformed back into the observer's frame depending on the beaming factor and the redshift. The observed photon energy $\varepsilon_{\text{obs}} = \varepsilon\mathcal{D}/(1+z)$, and the time duration $dt_{\text{obs}} = dt(1+z)/\mathcal{D}$.

3. Numerical Model of a Steady State

We use the observational data in Hartman et al. (2001). In particular, the spectral energy distribution (SED) observed between 1996 January 16 and 30 (P5a in their paper) is used for our model of a steady state. 3C 279 is in a preflare stage in this period and is not necessarily in a quiescent state. However, we fitted the data assuming that the spectrum is approximated by a steady state solution of the kinetic equations.

In Figure 1, our model is plotted with the observed data. We obtain the following values for the parameters: $\Gamma = 25$, $B = 0.3$ G, $R = 7 \times 10^{16}$ cm, $p = 1.8$, $\gamma_{\text{min}} = 4$, $\gamma_{\text{max}} = 1.8 \times 10^3$, the injection rate $2.3 \times 10^{-4} \text{ cm}^{-3}\text{s}^{-1}$, $\varepsilon_{\text{ext}} = 50$ eV, and $u_{\text{ext}} = 2 \times 10^{-4} \text{ ergs cm}^{-3}$. The spectrum below $\sim 10^{15}$ Hz is produced by synchrotron radiation, although the radio emission is probably from the outer regions of the jet. The radiation between 10^{16} and 10^{19} Hz is from synchrotron-self-Compton scattering, and the γ -rays above 10^{20} Hz are from the inverse Compton scattering of external soft photons. As shown in Figure 1 by the dashed line, the photons scattered by electrons with $\sim \gamma_{\text{min}}$ appear around 10^{20} Hz. Thus the flux around 10^{20} Hz is sensitive to the value of γ_{min} . However, because the data in this regime are mostly upper limits, the constraint on γ_{min} is weak.

Based on our numerical calculations, it is found that $u_{\text{kin}}/u_B = 36$, where u_{kin} is the energy density of nonthermal electrons and u_B is the magnetic energy density. We also find that the Poynting power is given by $L_{\text{Poy}} = \pi R^2 c u_B \mathcal{D}^2 = 1.03 \times 10^{45}$ ergs s^{-1} and that the kinetic power is given by $L_{\text{kin}} = \pi R^2 c u_{\text{kin}} \mathcal{D}^2 = 3.69 \times 10^{46}$ ergs s^{-1} . The dominance of the kinetic energy of nonthermal electrons over that of magnetic fields is the same as that for TeV blazars such as Mrk 421 and Mrk 501 (KTK).

In Figure 2, the electron spectrum for the SED shown in Figure 1 is presented. It is found that the electron spectrum is rather flat in the γ - $\gamma^2 n_e(\gamma)$ plot. This is because the cooling of high-energy electrons is inefficient, owing to the K-N effects (Blumenthal 1971). Note that the external photon energy in the blob frame is $\varepsilon' \sim \Gamma \varepsilon_{\text{ext}}$ and that the K-N effects become effective for electrons with $\gamma_{\text{K-N}} \sim m_e c^2 / \varepsilon' \sim 400$, which is less than γ_{max} . The spectral shape is contrary to the models often employed to fit the observed data of blazars, in which $n_e(\gamma) \propto \gamma^{-p}$ below a break energy γ_{br} and $n_e(\gamma) \propto \gamma^{-(p+1)}$ above γ_{br} ; the value of γ_{br} is determined by $t_{\text{cool}} = t_{e,\text{esc}}$, where t_{cool} is the electron cooling time. Nominally, γ_{br} is about 30. As seen in Figure 2, the actual spectral shape is much different from this conventional expectation. The flat γ -ray spectrum in $10^{21} - 10^{24}$ Hz in the ν - F_ν plot is the result of these K-N effects.

The optical depth for photon absorption against electron-positron pair production is calculated (Gould & Schröder 1967). The optical depth is much smaller than unity and γ -rays escape without absorption.

4. Flare

The time variability of emission spectra from blazars is quite common. 3C 279 also shows time variation from radio to γ -rays (e.g., Wehrle et al. 1998). To understand the jet formation mechanisms and particle acceleration processes, it is important to understand the mechanism that causes the time variability. Sikora et al. (2001) and Spada et al. (2001) show how flare light curves behave according to the shock-in-jet models, which assume that blobs with different speeds collide and that the kinetic energy of the bulk motion is dissipated. Ballo et al. (2002) interpreted the time variability of 3C 279 as being the result of various values of Γ , although they assumed a broken power-law spectrum of electrons without solving the kinetic equation.

We apply the internal shock model, by which Takahara et al. (2003) will explain the time variability of Mrk 421, to a flare observed from 3C 279. Without considering the details of the collision process, we simply assume that a coalesced blob has a bulk Lorentz factor Γ_f

and that various physical quantities scale with Γ . We examine whether or not the flares are explained by a change in Γ , keeping a constant opening angle for the jet cone. The distance of the collision location from the base of the jet, d , scales proportional to Γ^2 , while the lateral size of the observed region behaves as $R \propto \Gamma$, which is roughly equal to the shell thickness in the comoving frame, because the angle from the line of sight is limited by $\sim \Gamma^{-1}$. The soft photon energy density changes as $u_{\text{ext}} \propto \Gamma^2 d^{-2} \propto \Gamma^{-2}$. We assume that the kinetic and Poynting powers scale proportional to Γ^2 so that the total number flux remains constant. Thus, the injection rate in the comoving frame, q , scales proportional to $d^{-2} R^{-1} \propto \Gamma^{-5}$, and the magnetic field scales proportional to Γ^{-2} . We also assume γ_{min} and γ_{max} do not depend on Γ . The value of $\varepsilon'_{\text{ext}}$ scales proportional to Γ because of the Doppler effects. Using this scaling, we calculate a flare spectrum. Assuming that the spectrum shown in Figure 1 is in a quiescent state, the spectrum observed between 1996 January 30 and February 6 is fitted. Here the bulk Lorentz factor in Figure 1 is denoted as Γ_q , and that of a shocked blob is given by Γ_f . When $\Gamma_f = 1.6\Gamma_q = 40$, the γ -ray spectrum is fitted fairly well by our model (Figure 3), although there are some minor discrepancies: The slope in the optical-UV regime is slightly different; the flux between 10^{19} and 10^{20} Hz is underestimated; and the flux between 10^{20} and 10^{21} Hz is overestimated.

5. Summary and Discussion

We used the kinetic equations of photons and electrons to calculate emission spectra from 3C 279, assuming that the emission is from a relativistically moving blob almost along the line of sight. Our numerical solution shows that the γ -rays are produced by inverse Compton scattering of external soft photons, which is consistent with previous work (e.g., Inoue & Takahara 1996; Hartman et al. 2001; Ballo et al. 2002). However, we found that the electron spectrum is not a broken power law with a steeper spectrum above a break energy. Although electrons are cooled before escape (except those in the lowest energy range), the cooling efficiency for high-energy electrons decreases because of the K-N effects. As a result, a flat GeV γ -ray spectrum is obtained in the $\nu\text{-}\nu F_\nu$ plot. It should be noted that there is an alternative model of GeV emission that assumes different soft photon sources, i.e., the accretion disk and broad line regions (Hartman et al. 2001). In their model, because of the different temperatures of soft photons, a broad GeV emission is formed by inverse Compton scattering.

Our result of $\varepsilon_{\text{ext}} = 50$ eV seems to be a little high compared with the conventional value of around 10 eV. However, the spectra of ionizing radiation that form the broad line clouds are not directly constrained observationally but should extend to energy high enough to

multiply ionize atoms of heavy elements. From a theoretical point of view, even the emission from the accretion disk is known to deviate from the blackbody because of scattering effects. Thus, our choice may be suitable. Recently, it was suggested that IR radiation from dust might be important, if the energy dissipation occurs mainly far away from the central region (Błażejowski et al. 2000; Sikora et al. 2002); although we have not examined this case, the K-N effects will be weaker for this component.

The kinetic energy density of nonthermal electrons in the blob is an order of magnitude larger than the magnetic energy density, which is the same result as for TeV blazars (KTK). As a result, the particles transfer more energy in the jet from the central region to the outer region than the magnetic fields do.

We demonstrated that the flare observed between 1996 January 30 and February 6 is explained fairly well by the internal shock model with simple scaling laws described by a change in the bulk Lorentz factor. It is remarkable that the flare is fitted with those simple assumptions.

It was pointed out by Sikora & Madejski (2000) that the bulk motion of cold electrons/positrons in the jet scatters the external photons, resulting in observed emission peaking at energy $\varepsilon_{\text{BC}} \sim \Gamma^2 \varepsilon_{\text{ext}}$. Our model with $\Gamma = 25$ and $\varepsilon_{\text{ext}} = 50$ eV implies $\varepsilon_{\text{BC}} \sim 31$ keV ($\nu_{\text{BC}} \sim 7.5 \times 10^{18}$ Hz). The observed luminosity of bulk Compton (BC) scattering is estimated as

$$\begin{aligned}
 L_{\text{BC}} &\approx \Gamma^2 \int \left(\frac{4}{3} c \sigma_{\text{T}} u_{\text{ext}} \Gamma^2 \right) n_c dV \\
 &\approx 3.0 \times 10^{39} \left(\frac{\Gamma}{25} \right)^4 \frac{u_{\text{ext}}}{2 \times 10^{-4} \text{ ergs cm}^{-3}} \left(\frac{R}{7 \times 10^{16} \text{ cm}} \right)^3 n_c \text{ ergs s}^{-1},
 \end{aligned} \tag{4}$$

where σ_{T} is the Thomson cross section, n_c is the number density of cold electrons/positrons, and the integration is done over the blob volume. For 3C 279 with luminosity distance $d_L = 2.4 \times 10^3$ Mpc, where the Hubble constant $H_0 = 75 \text{ km s}^{-1} \text{ Mpc}^{-1}$ is assumed, νF_ν at ε_{BC} is $\sim L_{\text{BC}} / (4\pi d_L^2) \sim 7 \times 10^{-14} n_c / n_e \text{ ergs cm}^{-2} \text{ s}^{-1}$, where $n_e = 1.65 \times 10^4 \text{ cm}^{-3}$ is the number density of nonthermal electrons shown in Figure 2. The value of n_c / n_e is unknown, and unless it is about 100 or more, the BC spectrum is not observable; note that the observed value is $\sim 10^{-11} \text{ ergs cm}^{-2} \text{ s}^{-1}$ at $\varepsilon_{\text{BC}} \sim 31$ keV. Regions between the base of the jet and the blob may contribute to BC scattering because more cold electrons may exist there than in the blob. Let us assume that the bulk Lorentz factor is constant and that the number density of the cold electrons behaves as $n_c \propto \ell^{-2}$ for $\ell > \ell_0$, where ℓ is the distance from the central region and ℓ_0 is the critical distance where the bulk Lorentz factor saturates or the jet becomes optically thin. If we assume that u_{ext} scales proportional to ℓ^{-2} , the predicted value of L_{BC} is d/ℓ_0 times larger than that of equation (4), noting that $n_c dV$ is measured

in the comoving frame of the blob. Even if there are no cold electrons in the blob, in the inner-jet regions there should exist a corresponding number of cold electrons to relativistic electrons in the blob. Thus, we obtain the constraint of $\ell_0 > 0.01d$. If n_c/n_e in the blob is more than 100, too much BC emission is predicted, which probably means that u_{ext} does not increase much with a decrease in ℓ . In this case some modifications of our model are needed.

This work has been partially supported by Scientific Research Grants (M.K. and F.T.: 13440061; M.K.:15037210; F.T.: 14079205 and 14340066) from the Ministry of Education, Culture, Sports, Science and Technology of Japan.

REFERENCES

- Ballo, L, et al. 2002, ApJ, 567, 50
- Blandford, R. D., & Königl, A. 1979, ApJ, 232, 34
- Blumenthal, G. R. 1971, Phys. Rev. D, 3, 2308
- Błażejowski, M., Sikora, M., Moderski, R., & Madejski, G. M. 2000, ApJ, 545, 107
- Böttcher, M., & Chiang, J. 2002, ApJ, 581, 127
- Collmar, W. 2001, in The Universe in Gamma Rays, ed. Schönfelder, V. (Berlin: Springer), p. 285
- Coppi, P. S., & Blandford, R. D. 1990, MNRAS, 245, 453
- Crusius, A., & Schlickeiser, R. 1986, A&A, 164, L16
- Dermer, C. D., & Atoyan, A. M. 2002, ApJ, 568, L81
- Dermer, C. D., & Schlickeiser, R. 1993, ApJ, 416, 458
- . 2002, ApJ, 575, 667
- Georganopoulos, M., Kirk, J. G., & Mastichiadis, A. 2001, ApJ, 561, 111
- Ghisellini, G., & Madau, P. 1996, MNRAS, 280, 67
- Ghisellini, G., et al. 1998, MNRAS, 301, 451
- Gould, R. J., & Schréder, G. P. 1967, Phys. Rev., 155, 1404

- Hartman, R. C., et al. 2001, ApJ, 553, 683
- Inoue, S., & Takahara, F. 1996, ApJ, 463, 555
- Kino, M., Takahara, F., & Kusunose, M. 2002, ApJ, 564, 97 (KTK)
- Krolik, J. H. 1999, Active Galactic Nuclei (Princeton University Press: New Jersey)
- Kusunose, M., Takahara, F., & Li, H. 2000, ApJ, 536, 299
- Li, H., & Kusunose, M. 2000, ApJ, 536, 729
- Maraschi, L., et al. 1994, ApJ, 435, L91
- Mastichiadis, A., & Kirk, J. G. 1997, A&A, 320, 19
- Mukherjee, R., et al. 1997, ApJ, 490, 116
- Robinson, P. A., & Melrose, D. B. 1984, Australian J. Physics, 37, 675
- Sikora, M., Begelman, M. C., & Rees, M. J. 1994, ApJ, 421, 153
- Sikora, M., & Madejski, G. 2000, ApJ, 534, 109
- Sikora, M., & Błażejowski, M., Begelman, M. C., & Moderski, R. 2001, ApJ, 554, 1 (erratum 561, 1154)
- Sikora, M., & Błażejowski, M., Moderski, R., & Madejski, G. M. 2002, ApJ, 577, 78
- Spada, M., Ghisellini, G., Lazzatti, D., & Celotti, A. 2001, MNRAS, 325, 1159
- Takahara, F., Iwashimizu, C., Kino, M., & Kusunose, M. 2003, *in preparation*
- Thompson, D. J., et al. 1995, ApJS, 101, 259
- Ulrich, M.-H., Maraschi, L., & Urry, C. M. 1997, ARA&A, 35, 445
- Wehrle, A. E., et al. 1998, ApJ, 497, 178
- Xiao, F., Yabe, T., & Ito, T. 1996, Computer Physics Communications, 93, 1

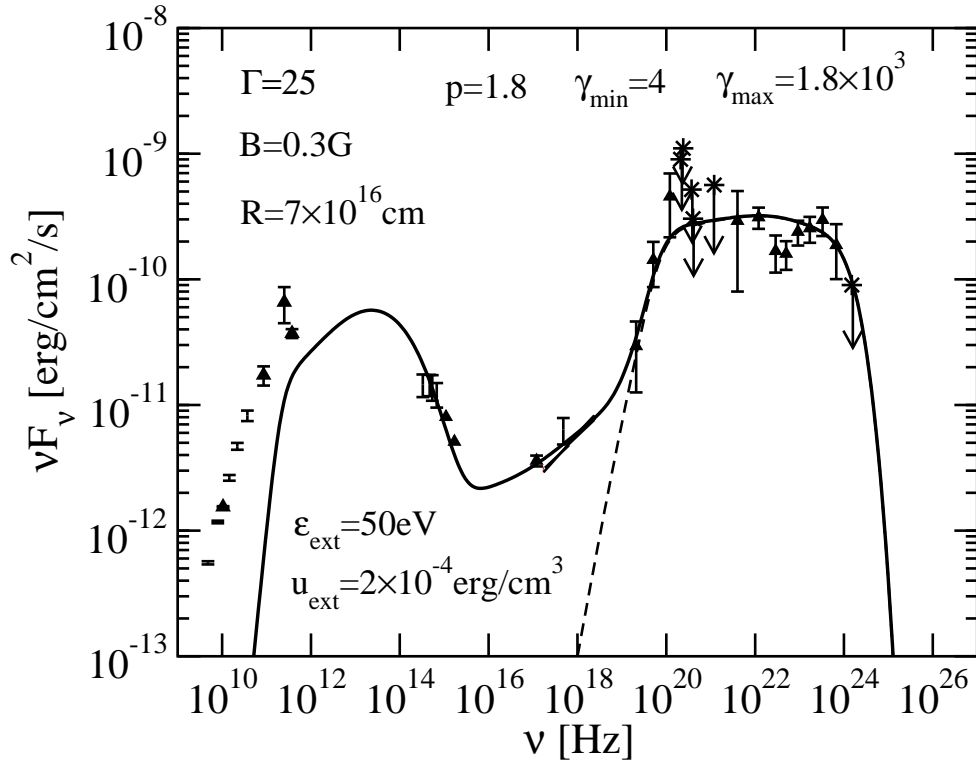


Fig. 1.— SED observed between 1996 January 16 and 30 with our model (*solid line*): The data are from Hartman et al. (2001). The values of the parameters are shown in the figure. The spectral component of EC scattering is shown by the dashed line.

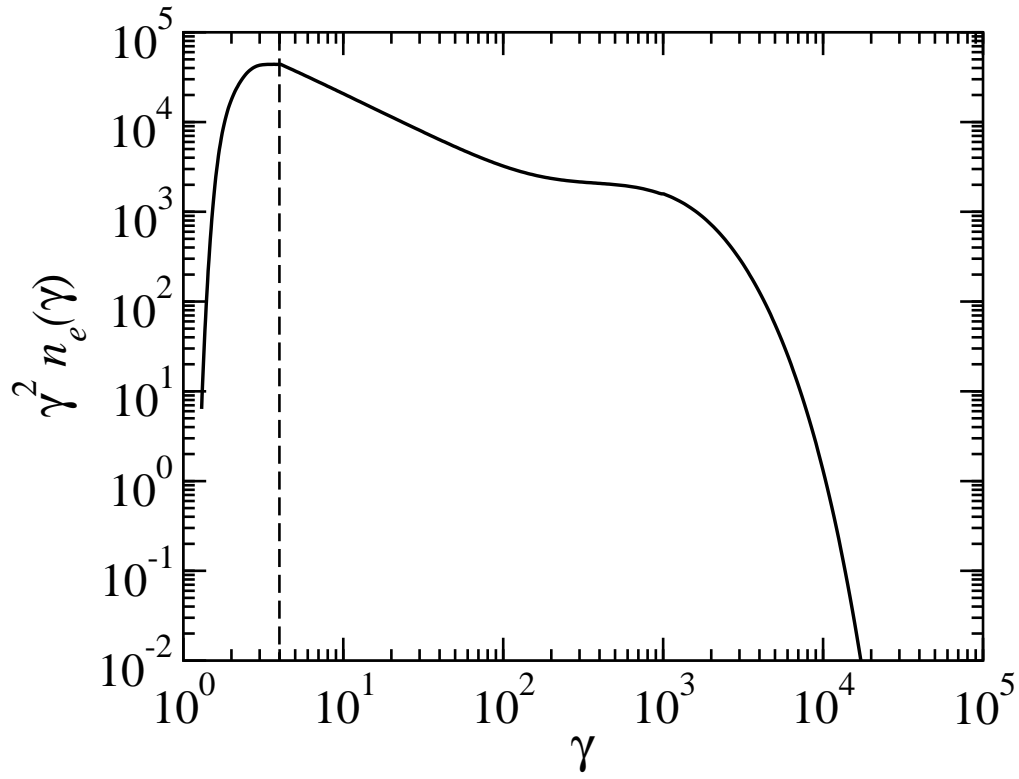


Fig. 2.— Electron spectrum for the SED shown in Figure 1. The vertical dashed line shows γ_{\min} . The spectrum is flatter above $\gamma \sim 100$ because of the K-N effects.

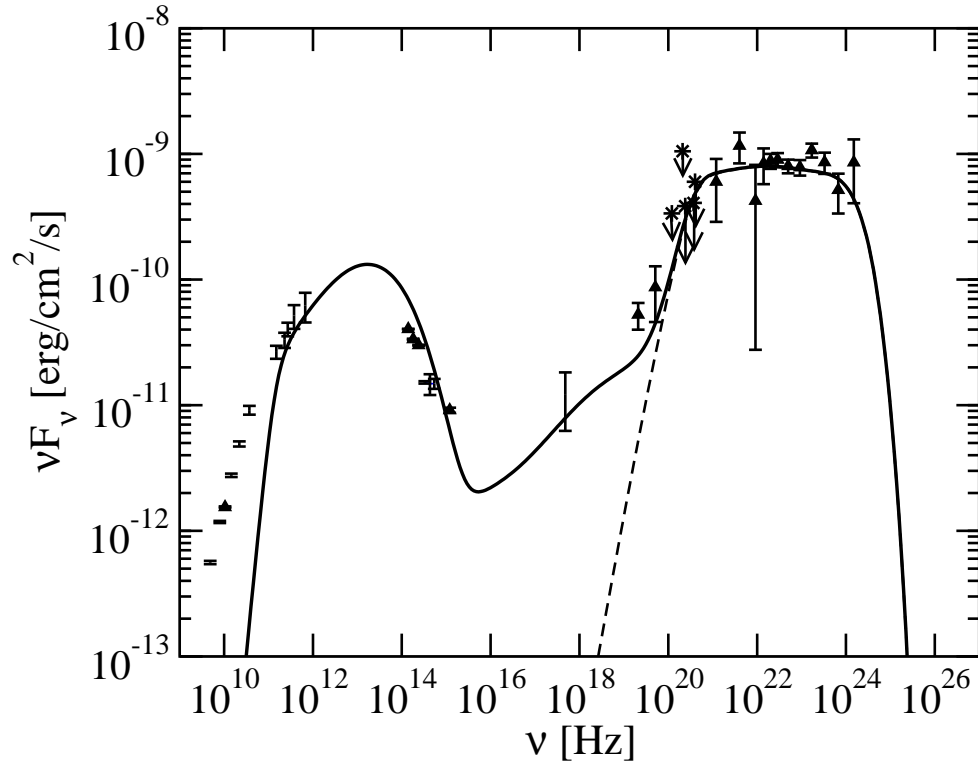


Fig. 3.— SED of the flare between 1996 January 30 and February 6. The solid line is calculated assuming $\Gamma_f/\Gamma_q = 1.6$. The spectral component of EC scattering is shown by the dashed line.